

# Determination of Stark Shifts and Widths Using Time Resolved Laser-Induced Breakdown Spectroscopy (LIBS) Measurements

Prashant Kumar , Swetapuspa Soumyashree,  
Nageswara Rao Epuru, Swaroop B Banerjee, R P Singh, and  
K P Subramanian

Applied Spectroscopy  
0(0) 1–8  
© The Author(s) 2020  
Article reuse guidelines:  
sagepub.com/journals-permissions  
DOI: 10.1177/0003702819891172  
journals.sagepub.com/home/asp



## Abstract

Stark broadening parameters have been estimated for resonant lines of Al(I) using time resolved measurements. The relation between the various emission line characteristics at different phases of opacity have been utilized to obtain the value of plasma temperature and Stark width parameters from the experimental data. The observed value of the center line intensity and Lorentzian component of the line width are compared against a simulated value of these parameters for optically thin case. The plasma temperature and Stark broadening parameters are obtained for the best fit condition by matching the experimentally observed and the simulated values of intensity and line widths. The time resolved measurements result in much better estimates for Stark parameters by allowing multiple points for fitting keeping the number of variables limited. The Stark shift parameters are also obtained from the slope of the plot of observed central wavelength shifts versus observed electron number density which is measured as a function of time. Hence, a method utilizing multiple-time observation data to obtain the Stark broadening parameters for lines showing self-absorption has been demonstrated.

## Keywords

Laser-induced breakdown spectroscopy, LIBS, stark widths, spectral line broadening, self-absorption

Date received: 10 October 2019; accepted: 25 October 2019

## Introduction

Laser-induced breakdown spectroscopy (LIBS) has emerged as an excellent tool for quantitative estimation and classification of samples under varied conditions.<sup>1–3</sup> A particular approach in LIBS, known as calibration free LIBS (CF-LIBS) utilizes the basic physics of the plasma processes to obtain the plasma parameters under the assumption of local thermodynamic equilibrium (LTE) condition for the plasma during the time of observation.<sup>4</sup> In order to calculate plasma parameters ( $T$ ,  $N_e$ , and  $C$ ), the LTE model require atomic parameters pertaining to the electronic energy levels involved in the transitions. Although most of these parameters (viz., partition functions, energy of levels, oscillator strengths, etc.) are readily available through various databases such as the National Institute of Standards and Technology (NIST)<sup>5</sup> or Kurucz,<sup>6</sup> there is a paucity of readily available data for Stark widths and shifts of various transitions for typical LIBS plasma conditions. As a result, in

most of the cases even though strong emissions are observed from those lines, they are not included in the analysis resulting in some uncertainty in the derived values of the parameters. Hence, to improve the results, it becomes important that the Stark parameters of such transitions are obtained.

Most of the theoretical estimates for Stark parameters of various transitions for different elements have been obtained following the work by Griem and others.<sup>7,8</sup> The theoretical data have been compared with various experimental observations and are reported in literature.<sup>9–11</sup> Most of the techniques for evaluating Stark parameters

Physical Research Laboratory, Ahmedabad, India

### Corresponding author:

Prashant Kumar, Physical Research Laboratory, Navrangpura, Ahmedabad 380009, India.

Email: prashantk@prl.res.in

using optical measurements of line widths assume that the plasma is optically thin and the self-absorption the emission line is negligible.

Lately, there have been attempts to obtain these parameters using LIBS for optically thin and thick plasma. Effect of various experimental factors on Stark parameter determination using LIBS, viz., acquisition time window, plasma inhomogeneity and self-absorption have been studied in detail by Bengoechea et al.<sup>12</sup> Temporal evolution of electron number density estimated from Stark broadening in aluminum plasma have been reported by Surmick and Parigger<sup>13</sup> which shows evidence of self-absorption. Stark broadening parameters for neutral and ionic Mn lines have been obtained by Bredice et al.<sup>14</sup> using LIBS measurements carried out at varying concentrations of Mn species in the plasma. Similar study for determining the Stark broadening parameter for a few Pb(II) lines at various time delays has been carried out by Alonso-Medina.<sup>15</sup> For optically thick plasma, determination of these parameters is performed after correcting the widths of the line for its self-absorption. Use of duplicating mirrors to calculate self-absorption in the plasma has been demonstrated by Moon et al.<sup>16</sup> and has been applied for Stark width estimation for a few Mg(I) and Mg(II) lines.<sup>17</sup> Another technique to estimate self-absorption is by utilizing the relation between the line intensity and its width using spectral radiance for optically thick plasma. The relation between various characteristics of emission line (viz., peak intensity, area under the curve and line widths) for optically thin and thick conditions have been discussed in detail by Amamou et al.<sup>18</sup> for different values of opacity. Similar techniques have been used by various groups to evaluate and correct for self-absorption in line intensities for quantitative estimation of elements.<sup>19–22</sup> While the previously mentioned techniques assume an LTE plasma, recently Liu et al.<sup>23</sup> have proposed a cross-calibration method in multielement samples to determine Stark parameters without relying on the LTE condition.

The present work for determining the Stark broadening parameter is based on the expressions derived by Amamou et al.<sup>18</sup> for spectral line parameters at different opacity values. Time resolved measurements have been utilized to compute these parameters at different opacities so as to obtain the value of Stark shifts and widths. From the experimentally observed value of line widths and electron number densities, a least square fitting is performed on the experimental value of line intensities computed for optically thin plasma to obtain temperature and the Stark parameters. As a demonstration of the developed scheme, it is applied to obtain the Stark parameters for the resonant lines of neutral Aluminum atom. Self-absorption in these lines have been extensively studied by different groups.<sup>24,25</sup> The results from the method proposed here have also been compared with the theoretical and experimental values reported elsewhere.

## Methodology

### Determination of Stark Widths

The present scheme to retrieve the Stark parameters is based on the assumption of homogeneous LTE plasma during the recording of LIBS spectrum. The line intensity from the plasma under this assumption can be written as<sup>18,20,26,27</sup>

$$I_{\lambda} = I_{\lambda}^{\dagger} \frac{1 - \exp(-\tau_{\lambda})}{\tau_{\lambda}} \quad (1)$$

where  $I_{\lambda}^{\dagger}$  is the line intensity for optically thin case and  $\tau_{\lambda}$  is the optical thickness of the plasma. The term,  $I_{\lambda}^{\dagger}$  in the above relation can be written as

$$I_{\lambda}^{\dagger} = F_{\lambda}^{inst} \frac{8\pi hc^2}{\lambda_0^5} \frac{n_j g_i}{n_i g_j} \tau_{\lambda} \quad (2)$$

In the above equation,  $F_{\lambda}^{inst}$  is the instrument factor consisting of the instrumental width, detector and collection efficiency, etc.,  $\lambda_0$  is central wavelength of the line emission involving an upper state  $j$  and lower state  $i$ . The terms,  $n_j$ ,  $n_i$ ,  $g_j$ , and  $g_i$  are the number densities and statistical weights of the respective upper and lower energy levels and  $\tau_{\lambda}$  can be written as

$$\tau_{\lambda} = \kappa_{\lambda} \times l_{abs} \quad (3)$$

where  $l_{abs}$  is the absorption path length and  $\kappa_{\lambda}$  is the opacity term given by

$$\kappa_{\lambda} = \frac{2e^2 n_i f \lambda_0^2}{mc^2} \times \frac{\Delta\lambda_L}{4(\lambda - \lambda_0)^2 + \Delta\lambda_L^2} \quad (4)$$

The electronic charge  $e$  in the above relation is in units of statcoulomb,  $f$  is the oscillator strength and  $\Delta\lambda_L$  is the full width half-maximum (FWHM) of the Lorentzian profile due to Stark broadening. In writing the above equation, it has been assumed that the opacity of the emission line under investigation is mainly governed by the Lorentzian component (Stark broadening) since Doppler broadening at typical temperatures under LIBS conditions is very less.<sup>20,25</sup>

Using Boltzmann distribution of electrons in different levels, number density in any level  $k$  can be written as

$$n_k = \frac{n_0 g_k}{U(T)} e^{-\frac{E_k}{k_B T}} \quad (5)$$

where  $U(T)$  is the partition function at temperature  $T$ ,  $n_0$  is the total number density and  $k_B$  is the Boltzmann constant.

The opacity term can be used to relate the line characteristics (peak intensity and line width) for optically thin and thick case. These relations can be derived from Eqs. 1, 3, and 4 and can be written as<sup>18</sup>

$$\frac{I_0}{I_0^{\dagger}} = \frac{1 - \exp(-\tau_0)}{\tau_0} \quad (6)$$

$$\frac{\Delta\lambda}{\Delta\lambda^\dagger} = \left[ -1 - \frac{\tau_0}{\log\left(1 + \frac{\exp(-\tau_0)}{2}\right)} \right]^{\frac{1}{2}} \quad (7)$$

where the terms with subscript 0 are computed at central wavelength, i.e.,  $\lambda = \lambda_0$ . Hence,  $[I_0, \Delta\lambda]$  and  $[I_0^\dagger, \Delta\lambda^\dagger]$  are the peak intensities and line widths for optically thick and thin case respectively.

The Stark width parameter,  $w_s$ , can be used to relate the line width as<sup>14,17,28,29</sup>

$$\Delta\lambda^\dagger = 2w_s \frac{n_e}{10^{16}} \quad (8)$$

where  $n_e$  is the electron number density in units of  $\text{cm}^{-3}$ .

Therefore,  $w_s$  can be obtained once  $\Delta\lambda^\dagger$  is known. From the experimental data, value of peak intensity,  $I_0$  can be directly obtained. The line width for optically thick plasma,  $\Delta\lambda$ , is obtained using numerical de-convolution of the Voigt profile after removing the instrument broadening from the experimentally recorded profile. To obtain  $\Delta\lambda^\dagger$  from the experimental spectrum, value of  $\tau_0$  needs to be obtained. As seen from Eqs. 3 to 5, this value not only depends on plasma temperature  $T$ , but on also on  $\Delta\lambda^\dagger$  itself. Hence a direct estimation of  $\Delta\lambda^\dagger$  or  $T$  is not possible.

The ratio of the line characteristics for optically thin and thick case, given by Eqs. 6 and 7, depend on the opacity value. A numerical computation of these two parameters at different value of opacity can hence be used to obtain relation between the parameters. For this, both these ratios were computed for different opacity values and the same is shown in Fig. 1. The obtained value of these ratios were then used to find a relation between these parameters. A functional form of type  $y = ax^b$  results in a best fit to the curve with  $a$  and  $b$  values as, 0.9822 and  $-1.753$

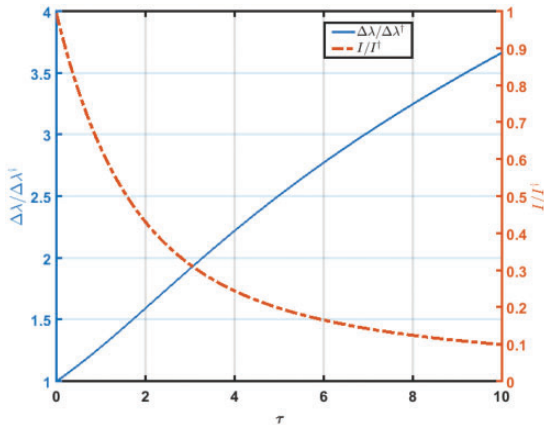


**Figure 1.** Evaluation of  $\frac{I_0}{I_0^\dagger}$  and  $\frac{\Delta\lambda}{\Delta\lambda^\dagger}$  at different values of optical thickness,  $\tau$ .

respectively.

$$\frac{I_0}{I_0^\dagger} = 0.9822 \times \left( \frac{\Delta\lambda}{\Delta\lambda^\dagger} \right)^{-1.753} \quad (9)$$

The fitted curve along with the numerically computed values are shown in Fig. 2. The maximum relative error after fitting is 1% using the above values of the parameters  $a$  and  $b$ . A similar value of the exponent  $b$  has been used in an iterative procedure suggested by Sherbini et al.<sup>25</sup> to obtain “true” line widths using self-absorption parameter relating the value of  $I_0/I_0^\dagger$  with  $\Delta\lambda/\Delta\lambda^\dagger$ . Using line integrated intensities for optically thin and thick cases, the method has also been applied by Praher et al.<sup>20</sup> in quantitative estimation of composition in oxide materials.

The present scheme utilizes this relation for comparing the experimentally observed quantities with numerically computed values of plasma temperature,  $T$  and  $\Delta\lambda^\dagger$  at different time intervals having different values of opacity. Hence, using the time data the computed values of  $\Delta\lambda^\dagger$  are better constrained. The procedure is explained as follows.

Equation 9 can be rearranged as

$$I_0(\Delta\lambda)^{1.753} = 0.9822 \times I_0^\dagger(\Delta\lambda^\dagger)^{1.753} \quad (10)$$

Using Eq. 10, by taking a ratio for a pair of lines and substituting for  $\Delta\lambda^\dagger$  from Eq. 8, we obtain

$$\underbrace{\frac{I_0}{I_0^{ref}} \left( \frac{\Delta\lambda}{\Delta\lambda^{ref}} \right)^{1.753}}_{Y_{obs}} = \underbrace{\frac{I_0^\dagger}{I_0^{\dagger ref}} \left( \frac{w_s}{w_s^{ref}} \right)^{1.753}}_{Y_{cal}} \quad (11)$$

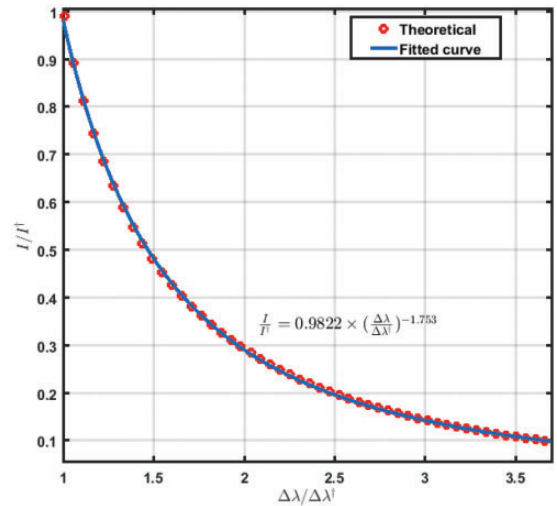


**Figure 2.** Relation between  $\frac{I_0}{I_0^\dagger}$  and  $\frac{\Delta\lambda}{\Delta\lambda^\dagger}$  obtained for different values of  $\tau$  as shown in Fig. 1.

The term on left can be obtained experimentally at different times and can be written as,  $Y_{obs}(t, \lambda_0)$ . The term on the right,  $Y_{cal}(T(t), n_e(t), w_s(\lambda_0))$  can be easily computed numerically using Eqs. 2 to 5 once the values for  $T(t)$ ,  $n_e(t)$  and  $w_s(\lambda_0)$  are known. Also note that by taking a ratio in Eq. 11, two unknown parameters i.e.,  $F_{inst}$  and  $I_{abs}$  have been eliminated from computation (see Eqs. 2 and 3). The error,  $\epsilon$  between these two parameters can be expressed as

$$\epsilon = Y_{obs}(t, \lambda_0) - Y_{cal}(T(t), n_e(t), w_s(\lambda_0)) \quad (12)$$

By performing a least square fitting to minimize the above error, one can obtain value of temperature at different times,  $T(t)$  and  $w_s(\lambda_0)$  for different  $\lambda_0$  provided the value of electron number density  $n_e(t)$  is known. The value of electron number density at different times is obtained using Stark broadening of the  $H_\alpha$  line present in the spectrum and is obtained as<sup>17</sup>

$$n_e(t) = 10^{17} \times \left( \frac{\Delta\lambda_{H_\alpha}(t)}{1.098} \right)^{1.47135} \quad (13)$$

As a special case of Eq. 11 which is relevant to the present study, the expression is hugely simplified if the lines involved belong to the same species and have identical or very similar value of upper state level energies and transition wavelength. For such cases, Eq. 11 can be simplified using Eq. 2:

$$\frac{I_0}{I_0^{ref}} \left( \frac{\Delta\lambda}{\Delta\lambda^{ref}} \right)^{1.753} = \frac{F_{\lambda}^{inst}}{F_{\lambda}^{ref}} \frac{gf}{(gf)^{ref}} \left( \frac{w_s}{w_s^{ref}} \right)^{0.753} \quad (14)$$

The term on the right is independent of temperature and number density and can be simply obtained from the experimentally obtained value mentioned in the left term. This simplification will be used later in our analysis.

To test the above method, synthetic spectrum for different values of  $n_e$  and  $T$  (to simulate time resolved measurements) for four resonant lines of aluminum, Table I, was numerically generated using the method discussed in our earlier work.<sup>27</sup> One such spectrum for  $T = 14000K$  and  $n_e = 1.0 \times 10^{18} \text{cm}^{-3}$  is shown in Fig. 3. As seen from Fig. 3, the lines are merged because of broadening due to Stark and self-absorption. For such cases, multiple Voigt profile fit was performed to retrieve the values of peak intensity and line widths as shown in the inset of Fig. 3. From the simulated spectrum,  $Y_{obs}$ , as mentioned in Eq. 11 was obtained for the four lines of Al(I) (308.2 nm, 309.2 nm, 394.4 nm, and 396.15 nm) using an ionic line, Al(II), 281.6 nm, as a reference. The atomic parameters for the reference ionic line were obtained from Kramida et al.<sup>5</sup> and Kurucz and Bell<sup>6</sup> and the Stark parameters were obtained from Konjevi et al.<sup>10</sup> and Fleurier et al.<sup>30</sup> The value of  $Y_{cal}$  was then obtained by varying  $T$  and  $w_s(\lambda_0)$  simultaneously so that the error in Eq. 12 is minimized. The value obtained for  $T$  and  $w_s(\lambda_0)$

**Table I.** Atomic data for the four Al(I) lines used in the present study.<sup>5,6</sup>

Wavelength (nm)	log (gf)	$E_i$ (cm <sup>-1</sup> )	$E_j$ (cm <sup>-1</sup> )
308.21	-0.447	0	32435.4
309.27	-0.187	112.06	32436.8
394.40	-0.623	0	25347.8
396.15	-0.323	112.06	25347.8

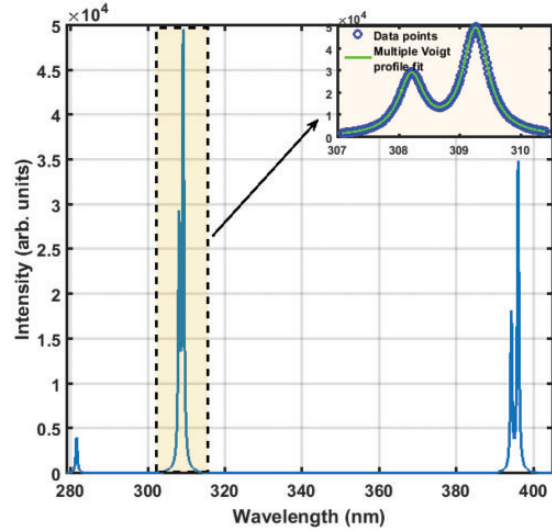


**Figure 3.** Synthetic spectrum for Al at  $T = 14000K$  and  $n_e = 1.0 \times 10^{18} \text{cm}^{-3}$  used to verify the method discussed in the text. Multiple Voigt profile fit to overlapping lines to retrieve the value of peak intensity, central wavelength and line width from the simulated spectrum is shown in the inset.

after fitting  $Y_{obs}$  with  $Y_{cal}$  perfectly matched with the input value resulting in a relative error always less than 1%.

### Determination of Stark Shifts

Obtaining Stark shifts in these lines are relatively simple with wavelength shifts,  $\delta\lambda$  depending on Stark shift parameter,  $d_s$  and  $n_e$  as<sup>17,28,29</sup>

$$\delta\lambda = d_s \frac{n_e(\text{cm}^{-3})}{10^{16}} \quad (15)$$

By obtaining shifts at various time delays, we can have plot of  $\delta\lambda(t)$  versus  $n_e(t)$ . From the slope of a straight line fit to this plot gives the value of Stark shift for the concerned line.

### Experimental

The LIBS experimental system used for the present study has been described in our previous work.<sup>27</sup> Briefly,

the system consists of neodymium-doped yttrium aluminum garnet (Nd:YAG) laser operating at fundamental frequency resulting in a power density of  $\sim 3 \times 10^{10} \text{ W/cm}^2$ . The light from the plasma is collected along the propagation axis through a collecting optics placed at a distance of  $\sim 15 \text{ cm}$  from the target and is fed to Echelle spectrometer (Andor) coupled with ICCD camera (Andor). The aluminum sample was mounted on a XYZ translation stage. The emission spectra were acquired starting from  $0.5 \mu\text{s}$  up to  $10 \mu\text{s}$  after plasma initiation at an interval of  $500 \text{ ns}$ . A photodiode (Thorlabs) was used to record the start time for the acquisition and all other trigger pulses were generated using digital delay generator (SRS). ICCD gate width was kept at  $500 \text{ ns}$  for all observations.

Wavelength calibration of the spectrometer was performed using Hg-Ar lamp. The accuracy of the wavelength calibration was estimated to be  $0.02 \text{ nm}$ . The instrumental broadening was also obtained from the Hg-Ar lamp in the wavelength region of interest. The instrument broadening contributes to the Gaussian shape with a width (FWHM) depending on the wavelength approximated by the following relation

$$\Delta\lambda_{\text{inst}} = 1.95 \times 10^{-4} \lambda(\text{nm}) + 0.0025 \quad (16)$$

The value is in agreement with the spectrometer specification of a resolving power of  $\sim 5000$ . The value of the calibration accuracy and the instrumental width are important since these play an important role in determining the Stark shift and the width parameter of the emission lines. The intensity calibration of the spectrometer along with other optical elements was performed using a Deuterium Halogen lamp (OceanOptics). For better repeatability, emission spectrum from 500 laser shots were averaged at each time interval and the sample was moved to a fresh location after every 20 shots.

## Data Analysis and Results

### Estimation of Lorentzian Widths and Electron Number Density

Experimental spectra obtained at times ( $t = 0.5 \mu\text{s}$  and  $5 \mu\text{s}$ ) are shown in Fig. 4 for reference. A piece-wise smoothening of the background intensity levels was performed for data acquired at lower time delay to remove the continuum from the data. A Voigt profile fitting routine based on Fourier expansion of complex error function<sup>31</sup> was used to obtain the Lorentzian component from the convoluted

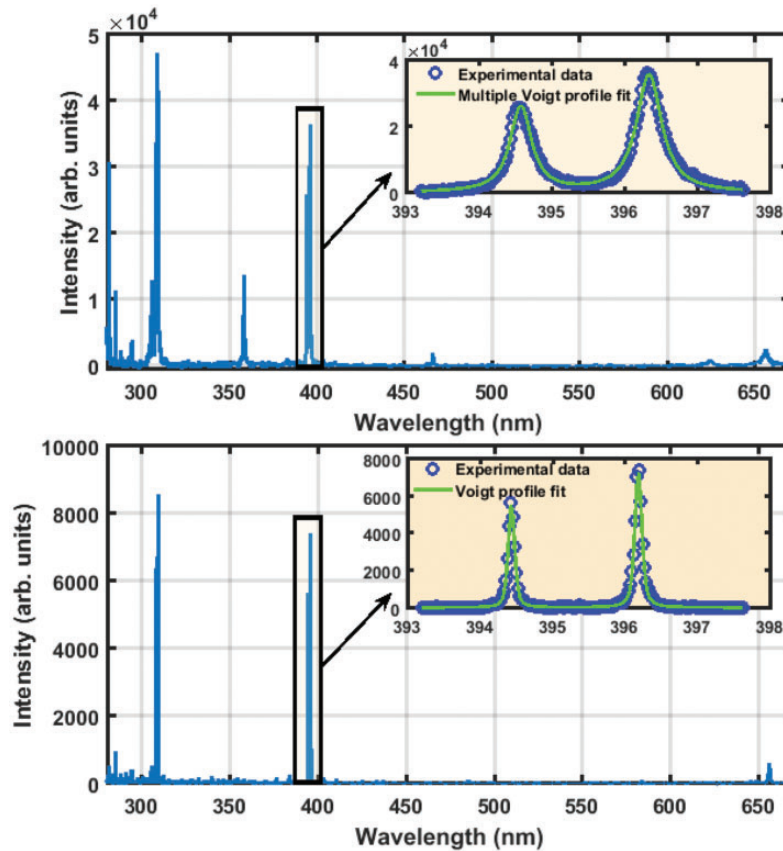


**Figure 4.** Experimental spectrum for Al at  $t = 0.5 \mu\text{s}$  (top panel) and  $5 \mu\text{s}$  (bottom panel). Voigt profile fit to two Al(I) lines appearing at  $394.4 \text{ nm}$  and  $396.15 \text{ nm}$  is shown in the inset of both the panels. Al(II) line appearing at  $281.6 \text{ nm}$  and  $H_{\alpha}$  line at  $656.3 \text{ nm}$  is also shown in the plot.



line profile. For this, instrumental broadening as given by Eq. 16 was used for the Gaussian part in the Voigt profile de-convolution. The Doppler broadening of the emission lines have been ignored in the present analysis as its value was found to be always less than 5% of the observed line widths. In cases where the lines are merged because of large broadening, multiple Voigt profiles were fitted to obtain the value of  $I$ ,  $\Delta\lambda$  and central wavelength,  $\lambda_0$  to be used in Eqs. 11 and 15 to obtain the Stark parameters. One such example is shown in the top panel of Fig. 4.

Temporal evolution of the Lorentzian widths of the four resonant emission lines of Al(I) considered in the present analysis were obtained as a result of fitting. For one of the lines, it is shown in Fig. 5. The value of electron number density was obtained using the relation mentioned in Eq. 13. Temporal evolution of  $n_e$  is also shown in Fig. 5.

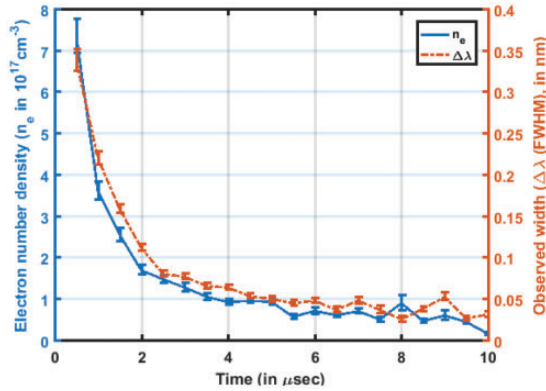


**Figure 5.** Temporal evolution of  $n_e$  and observed line width  $\Delta\lambda$  for  $\lambda_0 = 394.4$  nm. Also shown are the error values in  $n_e$  and  $\Delta\lambda$  as obtained from fitting.

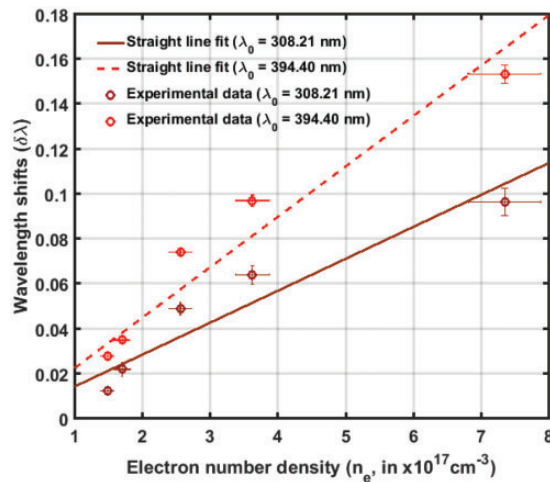


**Figure 6.** Plot of observed shifts versus electron number density,  $n_e$  along with the error bar in both the quantities for two Al(I) lines. Straight line fit is used to obtain the value of shift parameter. The values are reported in Table II.

## Estimation of Stark Parameters

**Stark Shifts.** The estimation of stark shifts is straightforward and is obtained using the method mentioned in the previous section. A plot of observed line shifts,  $\delta\lambda$  versus electron number density,  $n_e$  is shown in Fig. 6. Considering the calibration accuracy of the spectrometer as mentioned in previous section, data only up to  $2.5 \mu\text{s}$  was used for which the expected shifts are more than the accuracy of wavelength calibration. The Stark shift values obtained from the slope of the straight line shown in Fig. 6 are reported in Table II.

**Stark Widths.** Based on the value of Lorentzian component of the line width obtained after fitting,  $Y_{obs}$  as mentioned in Eq. 11, is calculated. The value of  $Y_{obs}$  is obtained using temporal data only up to a time delay when the instrumental width and observed Lorentzian widths are comparable

**Table II.** Stark shift parameter,  $d_s$  obtained for resonant lines of Al(I).

Wavelength (nm)	$d_s$ (in nm) Present work	$d_s$ (in nm) Literature
308.21	$0.0014 \pm 0.0004$	$0.0015^e$ , $0.0020^c$
309.27	$0.0014 \pm 0.0004$	$0.0015^e$ , $0.0020^c$
394.40	$0.0022 \pm 0.0004$	$0.0024^e$ , $0.0023^c$
396.15	$0.0024 \pm 0.0005$	$0.0024^e$ , $0.0023^c$

The experimental value (denoted with exponent e) are obtained from Fleurier et al.<sup>30</sup> and theoretical estimates (denoted with exponent c) are obtained from Dimitrijević and Sahal-Bréchet.<sup>32</sup>

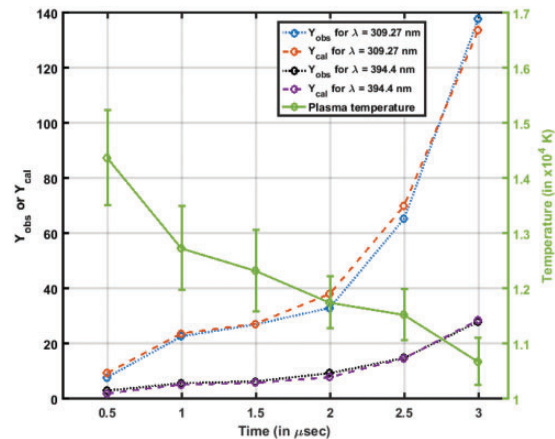


**Figure 7.** The values of  $Y_{obs}$  and  $Y_{cal}$  as a function of time as represented in Eq. 11. The time shown in the plot is the delay time at which the acquisition starts. The values of  $Y_{cal}$  shown in the figure are obtained for the best fit value of plasma temperature (green continuous line) and Stark width parameter for the set of four Al(I) line considered in the present study. The values obtained for Stark width parameter are reported in Table III.

**Table III.** Stark width parameter,  $w_s$  obtained for resonant lines of Al I.

Wavelength (nm)	$w_s$ (in nm) Present work	$w_s$ (in nm) Literature
308.21	$0.0029 \pm 0.0008$	$0.0043^c, 0.0045^e$
309.27	$0.0037 \pm 0.0011$	$0.0043^c, 0.0049^e$
394.40	$0.0021 \pm 0.0006$	$0.0029^c, 0.0037^e$
396.15	$0.0024 \pm 0.0007$	$0.0029^c, 0.0038^e$

The theoretically calculated values (denoted with exponent c) are obtained from Dimitrijević and Sahal-Bréchet<sup>32</sup> while experimental value (denoted with exponent e) are obtained from Roendigs and Kusch.<sup>33</sup>

so as to avoid fitting errors. Hence data only up to 3  $\mu$ s were used for this analysis. The values of  $Y_{cal}$  at different time  $t$  is a function of unknown variables  $T(t)$  and  $w_s$  which is fitted on to the  $Y_{obs}$  value using a least square fitting routine. Hence, the value of  $T$  and  $w_s$  are obtained for the best fit values. Note that the relation derived earlier for width parameters for a pair of lines having same or nearby upper energy level, Eq. 14, has been used in the analysis. The values of upper energy level for the set of lines considered in the present study are shown in Table I.

Plot of  $Y_{cal}$  and  $Y_{obs}$  as a function of time for two lines along with the plasma temperature value is shown in Fig. 7. The values of the Stark half width parameter derived from the experimental data for the four set of lines considered are shown in Table III. The values are also compared with data available in literature (Table III).

## Conclusion

By utilizing the relation derived for line emission parameters for optically thin and thick case, Stark broadening and shift parameters have been obtained for four resonant lines of neutral Aluminum. Line shifts observed at different timescales with varying electron number density is utilized to obtain the Stark shift parameter for these emission lines.

Experimental values of the line width and peak intensity obtained from time resolved LIBS measurement are used to obtain value of plasma temperature and Stark widths. The values of line emission parameters obtained experimentally are simultaneously fitted with the calculated values obtained for optically thin case. The advantage of this procedure is that the uncertainty in deriving the instrument factor and absorption path length in the line intensity relation no longer pose a challenge. The two terms automatically gets canceled by taking a simple ratio for any pair of lines. Of particular interest is the case when the set of lines belonging to a species have the same upper energy level. In such cases, it has been shown that the ratio of the Stark widths for the set of lines considered can be obtained directly from the experimental value of the line parameters even though they are self-absorbed. The obtained relation

has been utilized while retrieving the Stark broadening parameters using the experimental data for the set of lines considered.

The computations performed for data acquired at different plasma evolution times are akin to acquiring data at different opacity values. Hence, the relation obtained for emission line intensity and its width at different values of opacity is effectively used to obtain a better estimate of the derived broadening parameters.

## Declaration of Conflicting Interests

The author(s) declared no potential conflicts of interest with respect to the research, authorship, and/or publication of this article.

## Funding

The author(s) received no financial support for the research, authorship, and/or publication of this article.

## ORCID iD

Prashant Kumar  <https://orcid.org/0000-0001-7590-1311>

## References

1. J.D. Winefordner, I.B. Gornushkin, T. Correll, et al. "Comparing Several Atomic Spectrometric Methods to the Super Stars: Special Emphasis on Laser Induced Breakdown Spectrometry, Libs, A Future Super Star". *J. Anal. At. Spectrom.* 2004. 19: 1061–1083.
2. R.S. Harmon, R.E. Russo, R.R. Hark. "Applications of Laser-Induced Breakdown Spectroscopy for Geochemical and Environmental Analysis: A Comprehensive Review". *Spectrochim. Acta, Part B.* 2013. 87: 11–26.
3. L. Radziemski, D. Cremers. "A Brief History of Laser-Induced Breakdown Spectroscopy: From the Concept of Atoms to LIBS 2012". *Spectrochim. Acta, Part B.* 2013. 87: 3–10.
4. A. Ciucci, M. Corsi, V. Palleschi, et al. "New Procedure for Quantitative Elemental Analysis by Laser-Induced Plasma Spectroscopy". *Appl. Spectrosc.* 1999. 53(8): 960–964. (<http://as.osa.org/abstract.cfm?URI=as-53-8-960> [accessed Jan 25 2020]).
5. A. Kramida, Y. Ralchenko, J. Reader, et al. "NIST Atomic Spectra Database (ver. 5.3)". National Institute of Standards and Technology, Gaithersburg, MD, 2015, <http://physics.nist.gov/asd> [accessed Aug 24 2017].
6. R. Kurucz, B. Bell. "Atomic Spectral Line Database from CD-ROM 23 of R. L. Kurucz". Smithsonian Astrophysical Observatory, 1995, <https://www.cfa.harvard.edu/amp/ampdata/kurucz23/sekur.html> [accessed Jan 25 2020].
7. H. Griem. *Spectral Line Broadening by Plasmas*. St. Louis: Elsevier Science, 2014.
8. M. Dimitrijevic, S. Sahal-Brechot. "Stark Broadening of Al I Spectral Lines". *Phys. Scr.* 1994. 49: 34–38.
9. B. Martinez, F. Blanco. "Experimental and Theoretical Stark Width and Shift Parameters of Neutral and Singly Ionized Tin Lines". *J. Phys. B.* 1999. 32(2): 241–247.
10. N. Konjevi, A. Lesage, J.R. Fuhr, et al. "Experimental Stark Widths and Shifts for Spectral Lines of Neutral and Ionized Atoms (A Critical Review Of Selected Data for the Period 1989 through 2000)". *J. Phys. Chem. Ref. Data.* 2002. 31(3): 819–927.
11. C. Coln, G. Hatem, E. Verdugo, et al. "Measurement of the Stark Broadening and Shift Parameters for Several Ultraviolet Lines of Singly Ionized Aluminum". *J. Appl. Phys.* 1993. 73(10): 4752–4758.

12. J. Bengoechea, J. Aguilera, C. Aragn. "Application of Laser-Induced Plasma Spectroscopy to the Measurement of Stark Broadening Parameters". *Spectrochim. Acta, Part B*. 2006. 61(1): 69–80.
13. D.M. Surmick, C.G. Parigger. "Electron Density Determination of Aluminium Laser-Induced Plasma". *J. Phys. B At. Mol. Opt. Phys.* 2015. 48(11): 115701.
14. F. Bredice, F. Borges, H. Sobral, et al. "Measurement of Stark Broadening of Mn I and Mn II Spectral Lines in Plasmas Used for Laser-Induced Breakdown Spectroscopy". *Spectrochim. Acta, Part B*. 2007. 62(11): 1237–1245.
15. A. Alonso-Medina. "Measurement of Laser-Induced Plasma: Stark Broadening Parameters of Pb(II) 2203.5 and 4386.5 Å Spectral Lines". *Appl. Spectrosc.* 2019. 73(2): 133–151.
16. H.Y. Moon, K.K. Herrera, N. Omenetto, et al. "On the Usefulness of a Duplicating Mirror to Evaluate Self-Absorption Effects in Laser Induced Breakdown Spectroscopy". *Spectrochim. Acta, Part B*. 2009. 64(7): 702–713.
17. M. Cveji, M. Gavrilovi, S. Jovievi, et al. "Stark Broadening of Mg I and Mg II Spectral Lines and Debye Shielding Effect in Laser Induced Plasma". *Spectrochim. Acta, Part B*. 2013. 85: 20–33.
18. H. Amamou, A. Bois, B. Ferhat, et al. "Correction of Self-Absorption Spectral Line and Ratios of Transition Probabilities for Homogeneous and LTE Plasma". *J. Quant. Spectrosc. Radiat. Transf.* 2002. 75(6): 747–763.
19. D. Bulajic, M. Corsi, G. Cristoforetti, et al. "A Procedure for Correcting Self-Absorption in Calibration Free-Laser Induced Breakdown Spectroscopy". *Spectrochim. Acta, Part B*. 2002. 57(2): 339–353.
20. B. Praher, V. Palleschi, R. Viskup, et al. "Calibration Free Laser-Induced Breakdown Spectroscopy of Oxide Materials". *Spectrochim. Acta, Part B*. 2010. 65(8): 671–679.
21. C. Gerhard, J. Hermann, L. Mercadier, et al. "Quantitative Analyses of Glass via Laser-Induced Breakdown Spectroscopy in Argon". *Spectrochim. Acta, Part B*. 2014. 101: 32–45.
22. F. de Oliveira Borges, J.U. Ospina, G. de Holanda Cavalcanti, et al. "CF-LIBS Analysis of Frozen Aqueous Solution Samples by Using a Standard Internal Reference and Correcting the Self-Absorption Effect". *J. Anal. At. Spectrom.* 2018. 33: 629–641.
23. H. Liu, B.S. Truscott, M.N.R. Ashfold. "Determination of Stark Parameters by Cross-Calibration in a Multi-Element Laser-Induced Plasma". *Sci. Rep.* 2016. 6: 25609.
24. H. Amamou, A. Bois, B. Ferhat, et al. "Correction of the Self-Absorption for Reversed Spectral Lines: Application to Two Resonance Lines of Neutral Aluminium". *J. Quant. Spectrosc. Radiat. Transf.* 2003. 77(4): 365–372.
25. A.E. Sherbini, T.E. Sherbini, H. Hegazy, et al. "Evaluation of Self-Absorption Coefficients of Aluminum Emission Lines in Laser-Induced Breakdown Spectroscopy Measurements". *Spectrochim. Acta, Part B*. 2005. 60(12): 1573–1579.
26. W. Lochte-Holtgreven. *Plasma Diagnostics*. Amsterdam: North-Holland Publishing Company, 1968.
27. P. Kumar, R.K. Kushawaha, S.B. Banerjee, et al. "Quantitative Estimation of Elemental Composition Employing a Synthetic Generated Spectrum". *Appl. Opt.* 2018. 57(19): 5443–5450.
28. N. Konjevi. "Plasma Broadening and Shifting of Non-Hydrogenic Spectral Lines: Present Status and Applications". *Phys. Rep.* 1999. 316(6): 339–401.
29. M. Ivkovi, N. Konjevi. "Stark Width and Shift for Electron Number Density Diagnostics of Low Temperature Plasma: Application to Silicon Laser Induced Breakdown Spectroscopy". *Spectrochim. Acta Part B At. Spectrosc.* 2017. 131: 79–92.
30. C. Fleuri, S. Sahal-Brechot, J. Chapelle. "Stark Profiles of Al I and Al II Lines". *J. Phys. B At. Mol. Opt. Phys.* 1977. 10(17): 3435–3441. (doi:10.1088/0022-3700/10/17/018. <https://doi.org/10.1088/0022-3700/10/17/018> [accessed Jan 25 2020]).
31. S. Abrarov, B. Quine, R. Jagpal. "Rapidly Convergent Series for High-Accuracy Calculation of the Voigt Function". *J. Quant. Spectrosc. Radiat. Transf.* 2010. 111(3): 372–375.
32. M.S. Dimitrijević, S. Sahal-Brechot. "Stark Broadening of Al I Spectral Lines". *Phys. Scr.* 1994. 49(1): 34–38.
33. G. Roendigs, H.J. Kusch. "Electron Impact Broadening of Aluminum I-Lines". *Astron. Astrophys.* 1979. 71: 44–46.